IEEE Access
Multidisciplinary | Rapid Review | Open Access Journal

Received March 3, 2021, accepted March 22, 2021, date of publication March 30, 2021, date of current version April 7, 2021.

Digital Object Identifier 10.1109/ACCESS.2021.3069676

Real-Time Implementation of Extended Kalman Filter Observer With Improved Speed Estimation for Sensorless Control

MOHANA LAKSHMI JAYARAMU[1], (Senior Member, IEEE), H. N. SURESH[1], MAHAJAN SAGAR BHASKAR[2], (Senior Member, IEEE), DHAFER ALMAKHLES[2], (Senior Member, IEEE), SANJEEVIKUMAR PADMANABAN[3], (Senior Member, IEEE), AND UMASHANKAR SUBRAMANIAM[2], (Senior Member, IEEE)

[1]Department of Electrical and Electronics Engineering, Malnad College of Engineering, Hassan 573202, India
[2]Renewable Energy Laboratory, Department of Communication and Networks, College of Engineering, Prince Sultan University (PSU), Riyadh 11586, Saudi Arabia
[3]CTiF Global Capsule, Department of Business Development and Technology, Aarhus University, 7400 Herning, Denmark

Corresponding authors: Mohana Lakshmi Jayaramu (mohana2024@gmail.com) and Mahajan Sagar Bhaskar (sagar25.mahajan@gmail.com)

This work was supported by the Renewable Energy Laboratory (REL), Department of Communications and Network Engineering, College of Engineering, Prince Sultan University, Riyadh, Saudi Arabia.

ABSTRACT This work presents an investigation on Improved Extended Kalman Filter (IEKF) performance for induction motor drive without a speed sensor. The performance of a direct sensorless vector-controlled system through simulation and experimental work is tested. The proposed observer focuses on estimating rotor flux and mechanical speed of rotor from the stationary axis components. Extended Kalman Filters' estimation performance depends on the system matrix's proper value (Q) and measurement error matrix (R). These matrices are assumed to be persistent and are calculated by the trial-and-error method. But, the operating environment affects these matrix values. They must be updated based on the prevailing operating conditions to get high speed and accurate estimates. The values of Q and R in the Improved EKF (IEKF) algorithm are obtained using the genetic algorithm. Besides, IEKF is incorporated to reduce in computational burden for real-time applications.

INDEX TERMS Extended Kalman filter, inductor motor, real-coded-genetic algorithm, sensorless drives, speed estimator.

I. INTRODUCTION

For precise control of Induction Motors (IMs), values of speed, torque, rotor & stator fluxes have to be accurately estimated. In the past decade, model-based methods of IM using notations of space vector were developed. The information needed for the model-based approach is obtained by measuring the voltage and current at machine terminals. But, these model-based methods were observed to be very sensitive to machine parameters. Model-based methods need past information on the motor's electrical parameters and characteristics. Different IM parameters are measured at standstill and speed, and the current controller is tuned accordingly; the machine changes parameters during normal operation. The parameters that change during normal operation are due to thermal conditions. There are changes in rotor and stator resistances; the inductance parameters depend on the flux level's value. Also, the values of leakage co-efficient change as flux and load vary. Over the last few years, there is an increased interest in applying the speed sensorless Field Oriented Control (FOC) method to high-performance IM applications. It bases this on computing the speed using machine via's parameters, the instantaneous value of current and voltage in stator [1], [2]. Also, few Adaptive Observers, namely Luenberger observer/Extended Kalman Filter (EKF) [3], [4] provide accurate speed estimates under de-tuned operating conditions. Comprehensive reviews on the sensorless drive via model-based computation methods failed to assure the machine's stability [5]. The drive systems are susceptible to inaccuracy and variations in motor equivalent circuit parameters. This may induce errors that degrade the speed holding characteristics. It intensifies the problem,

The associate editor coordinating the review of this manuscript and approving it for publication was Zhuang Xu.

due to unbalanced motor winding or any DC offset present in current controllers. Unwanted DC offset can be eradicated by auto-calibration of DC link current. [6], [7].

Various methods have been proposed over the last few decades for speed estimation and control of IM. Conventional speed estimation techniques include the MRAS [8], derivatives of rotor flux [9], [10], voltages in stator [11], a modified version of stator model, full order observer [11], [12], unscented extended Kalman filter [13], reduced-order non-linear observer [14], [15], Extended Kalman filter observer assisted with fuzzy optimization [16], sliding mode observer [17], [18]. Few other speed estimators that don't depend on measured values of voltage and current are Artificial intelligent (AI) based neural networks [19], [20], harmonic rotor slotting [21], [22], high-frequency signal injection [21]–[23]. These investigations [9]–[23] involve closed-loop strategies that use speed estimation techniques, considering the IM model to be linear. However, IM is a non-linear machine and requires accurate parameter estimation techniques and a robust speed control method. The advancements in technology, fast computing processors have led to robust speed estimation schemes. These works let to the development of the Bi-Input Extended Kalman Filter estimation method. But these methods have been shown to use more time to determine the noise covariance matrix's proper values [24]–[29]. Neuro-fuzzy techniques were applied for performance enhancement of the drive [28]–[30]. The work reported involves AI techniques using a state observer, which includes an adaptive intelligent technique using human knowledge and fuzzy-based systems. In [30], [31], new machine drive techniques are explained through other estimation methods to measure very low-speed. A shaft encoder is used to calculate both speed and load torque disturbances. The values of temperature and uncertainties in frequency are also required for accurate flux and velocity computation in sensorless control [32]–[35]. Lyapunov's theorem has proved the stability of the adaptive schemes used for speed estimation, and results obtained through simulation are analyzed [36]. The estimation of stator resistance using EKF by realizing Field Programming Gate Array (FPGA) and IM operation at very low and near zero speed areas [37]. They introduce the implementation of EKF with a fading term in the covariance matrix and hence tune the gain matrix [38]. Investigations on optimizing the performance of EKF through speed and torque fitness functions for direct torque-controlled machines are provided in [39]. For improving the robustness of the speed estimator and control system against parameter uncertainties, and improved EKF scheme is developed that rests on the correct choice of 'System and Measurement covariance matrices'.

The estimation performance of Standard EKF is observed to deteriorate at low speed, transients, and under variations in equivalent circuit parameters. A real-coded integer Genetic Algorithm with improved precision using a new concept of the chromosome was reported in [40]. It optimizes the EKF with different values of fitness functions for speed-sensorless control of IM. The work has reported real-time experiments to state the best fitness function for accurate motion control [41]. Differential Evolution Algorithm is implemented to optimize the covariance matrices of reduced-order Kalman Filter in offline mode and realize the sensorless control of induction motors [42]. Also, the use of differential evolution algorithm for optimizing EKF is studied in [43]. This method, however, cannot address the sensitivity of the observer to stator resistance variations. Performance of GA-optimized EKF of constant V/Hz controller considering variation in parameters is proposed and implemented [44]. As speed sensorless control applications to induction motors are predominantly increasing, especially in EV applications, IM's dynamic performance for several speed profiles and different load torque disturbance conditions is to be achieved. The proposed research work intends to identify IM parameters considering the associated non-linearities and achieve improved speed estimation and control over an extensive speed zone. The effect of stator resistance and sensitivity of observer to variations in resistance of stator [43] is investigated.

In this research work, an improved Extended Kalman filter for control of induction motor in sensorless mode is performed. The values of the system (Q) and measurement (R) matrices are updated in Improved EKF (IEKF) algorithm using the genetic algorithm. The performance of sensorless vector-controlled drive systems is tested through simulation and experimental work. Earlier research investigations have focused on the estimation of rotor speed under different constraints. However, there is a need to address the vector control scheme for achieving good dynamic performance. Hence, in this research, the Bus Clamped Space Vector Modulation scheme is implemented, which has improved the IM drive system's complete performance. Re-configurability of Digital Signal Processing (DSP) devices gives researchers the chance to test and validate a novel controller; which does not damage the actual system through co-simulation, also known as Rapid Control Prototyping (RCP). The present work uses the Code Composer Studio (CCS) environment [45] to establish and validate an adaptive Improved Extended Kalman Filter (IEKF) speed estimator based on a Real-Coded-Genetic Algorithm (RC-GA-EKF). The research work models the system to improve the direct rotor field-oriented or the vector-controlled speed sensorless induction motor.

The paper is organized as: Section II presents the parameter estimation using an extended Kalman filter algorithm with a modified machine model. Section III describes the basic idea of Tuning Q & R Matrices Using Real-Coded-Genetic Algorithm (RC-GA). Section IV presents the hardware configuration of the process of EKF using RC-GA. The experimental and simulation results with suitable discussion are shown in section V. Finally, conclusions in section VI.

II. PARAMETER ESTIMATION WITH EXTENDED KALMAN FILTER

An improved speed computation scheme using a Genetic Algorithm based Extended Kalman Filter (EKF) is proposed.

EKF is considered a recursive estimator with optimum stochastic characteristics. A full order state observer is used in the state-space model to estimate the components viz., the flux of rotor, rotor speed, and stator current. This approach significantly reduces the execution time and simplifies the tuning of the covariance matrix. The fundamental steps to speed estimation using EKF include discretizing the machine model. For determining state and noise covariance matrices, and implementing and tuning the discretized EKF algorithm using real coded Genetic Algorithm to get proper rotor speed.

A. DISCRETISED STATE SPACE MODEL OF INDUCTION MOTOR

There are 4 state variables: stator currents in d & q axes (i_{ds}, i_{qs}) and the rotor fluxes (Φ_{dr}, Φ_{qr}) in the dynamic model of 3-phase IM. Including the rotor speed ω_r as an additional variable a modified model of IM results [40]. The discretized extended model is as got [39].

$$\begin{cases} X(n+1) = A \times \widehat{X}(n) + B \times U(n); Y(n) = \mathrm{C} \times X(n) \\ \widehat{X}(n) = \left[i^s_{ds}(n) \quad i^s_{qs}(n) \quad \phi^s_{dr}(n) \quad \phi^s_{qr}(n) \quad \omega_r(n) \right]^T \\ Y(n) = \left[i^s_{ds}(n) \quad i^s_{qs}(n) \right]^T \\ U(t_k) = \left[v^s_{ds}(n) \quad v^s_{qs}(n) \right]^T \end{cases} \tag{1}$$

where,

$$A = \begin{bmatrix} 1 - \frac{Z}{Z^*_s} & 0 & \frac{ZL_m}{L'_s L_r \tau_r} & \frac{\omega_r Z L_m}{L'_s L_r} & 0 \\ 0 & 1 - \frac{Z}{T^*_s} & \frac{-\omega_r Z L_m}{L'_s L_r} & \frac{ZL_m}{L'_s L_r \tau_r} & 0 \\ \frac{ZL_m}{L'_s L_r \tau_r} & 0 & 1 - \frac{Z}{Z^*_s} & -\omega_r Z & 0 \\ 0 & \frac{ZL_m}{\tau_r} & \omega_r Z & 1 - \frac{Z}{Z^*_s} & 0 \\ 0 & 0 & 0 & 0 & 1 \end{bmatrix}$$

$$B = \begin{bmatrix} \frac{Z}{L'_s} & 0 & 0 & 0 & 0 \\ 0 & \frac{Z}{L'_s} & 0 & 0 & 0 \end{bmatrix},$$

$$C = \begin{bmatrix} 1 & 0 & 0 & 0 & 0 \\ 0 & 1 & 0 & 0 & 0 \end{bmatrix}$$

and $\tau_r = \frac{L_r}{R_r}$; $\quad Z = R_s + \frac{L_m R_r}{L_r^2}$; $\quad Z^* = \left(1 - \frac{L_m^2/L_r}{L_s}\right) * L_s$

But, for an IM, the values of R_r, R_s, L_r, L_s, L_m, and ω_r are constant. Therefore, matrices of state vector input and output are taken as constant.

B. EXTENDED KALMAN FILTER ALGORITHM

With the modified model of induction motor, it is noticed that the state-space model is not linear. This is because it has self-product terms of the state variables. The method's essence stems from the linearization of the non-linear model, so use the system's first derivatives and written the filter structure according to this. The EKF is a recursive procedure that helps produce estimations of unknown variables using a series of measurements observed over time more precisely [40]. The EKF uses a non-linear model and observations and assumes error propagation to be linear. The other non-linear parameters are linearized. In the proposed method, we have attempted to develop the estimator to give improved performance using d-q axes stator current and flux values. The rotor speed is estimated via the reference speed added as a state variable and further tuning the EKF algorithm using a real coded Genetic Algorithm. The estimates are got by EKF as stated below:

- *State Vector Prediction*

This vector is predicted with a sampling interval of $(n+1)$. The value is obtained from input vector U(n), state vector, matrices A, and B.

$$X(n+1) = A \times \widehat{X}(n) + B \times U(n) \tag{2}$$

The values of matrices $\hat{X}(n), U(n), A, B$ can be got from (1),

- *Estimation of the Prediction Covariance matrix*

$$P^*(n+1) = \frac{\partial}{\partial x}[AX + BU]P(n)[\frac{\partial}{\partial x}[AX + BU]]^T + Q \tag{3}$$

The covariance matrix has the order of 5×5. A gradient matrix f can represent the terms in (3) as,

$$\frac{\partial}{\partial x}[AX + BU] = f(n+1) \tag{4}$$

where, $X = X^*(n+1)$

- *Computing Kalman filter gain value*

The order of gain matrix of the filter is taken as 2×5, and it is calculated as:

$$K(n+1) = \begin{bmatrix} P^*(n+1)[\frac{\partial}{\partial x}[CX]]^T \times \\ [\frac{\partial}{\partial x}[CX]P^*(n+1)[[\frac{\partial}{\partial x}[CX]]^T + R]^{(-1)}] \end{bmatrix} \tag{5}$$

where parameter CX is another gradient matrix represented by h as follows.

$$\frac{\partial}{\partial x}[CX] = h(n+1) \tag{6}$$

where $X = X^*(n+1)$

- *Estimating state vector*

Correct estimation of state estimator is done at the time interval $(n+1)$ and is done as given,

$$\begin{cases} \widehat{Y}(n+1) = CX^*(n+1) \\ \widehat{X}(n+1) = X^*(n+1) + K(n+1) \\ \qquad \left[Y(n+1) - \widehat{Y}(n+1) \right] \end{cases} \tag{7}$$

- Error covariance matrix

This matrix is attained as,

$$\widehat{P}(n+1) = P^*(n+1) - K(n+1) \left[\frac{\partial}{\partial x}[CX] \right] P^*(n+1) \tag{8}$$

- Updating parameters is done as follows:

$$X(n) = X(n-1), \quad k = (n+1) \ \textit{and}$$
$$P(n) = P(n-1) \tag{9}$$

In (2)-(9), ^refers to the estimated value, and * refers to the prediction parameter. Updated the algorithm with the values arrived through the (2)-(9) and develops covariance matrix that is modified upon iterations, and accurate estimates of the states are obtained by a trial-and-error method. Getting a faster response through correct tuning of Q and R matrices. An improvisation in the observer's performance is done in the present work using a real coded genetic algorithm that tunes matrices Q and R and gets accurate and quicker speed estimates.

III. TUNING OF Q AND R MATRICES USING REAL- CODED GENETIC ALGORITHM

In this study, the EKF algorithm is taken as an improved current model-based observer where it can provide very low-speed and high-speed zone operation. But, the values of filters affect the performance of estimated state vectors. Hence, in this work, a Real Coded Genetic Algorithm (RC-GA) optimizes the EKF observer and, in turn, helps optimize the controller's multi-dimensional performance.The primary aim is the minimization of error which is the mean squared value of the speed estimate $E_1(x)$ which is given by,

$$\begin{cases} E_1(x) = \dfrac{1}{n}\sum_1^n (\omega_{re} - \widehat{\omega}_{re}) \\ \omega_{re} \rightarrow \textit{actual speed}; \\ \quad \widehat{\omega}_{re} \rightarrow \textit{estimated speed from EKF} \end{cases} \tag{10}$$

where n is the sampling time, for improved speed estimate through EKF, three of its initializes matrices. It will update the covariance matrix P at each sample period of EKF iterations (10). Hence, only Q and R are optimized. Thus, RC-GA is employed, and the corresponding algorithm flow diagram is as in Fig. 1. The RC-GA for EKF (RC-GA-EKF) is implemented using MATLAB. For tuning the matrices Q and R of IEKF for vector control, parameters of RC-GA are set as follows:

- The initial population size : 100
- The maximum number of generations : 20
- The probability of crossover : 0.8
- The mutation probability : 0.1
- The initial range of real coded strings : [.1; 5]
- The performance measure : MSE obtained from the actual speed of the motor and estimated speed.

The selection of RC-GA parameters used to identify the vector P and hence tune Q and R of IEKF is as given above. The steps followed for implementing the RC-GA algorithm is given:

1) The five diagonal elements which are the decision variables representing the population index are ($q_{11}, q_{22}, q_{33}, q_{44}$, and q_{55}) of Q matrix, and the elements (r_{11}, r_{22}) are a diagonal

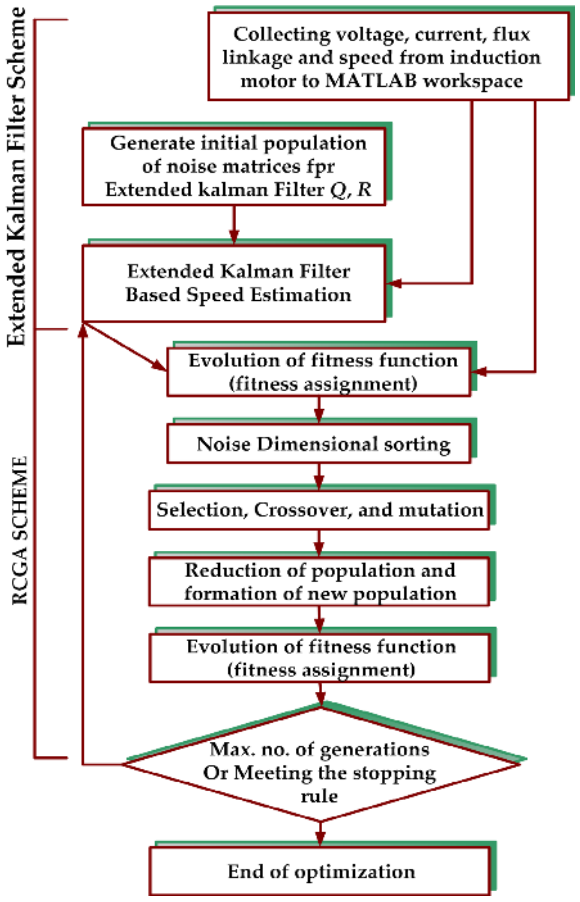

FIGURE 1. Flow diagram of RC-GA- EKF process.

representation of the R matrix. These are taken as a long string and coded further than shown below:

$$G = \begin{bmatrix} q_{11} & 0 & 0 & 0 & 0 \\ 0 & q_{22} & 0 & 0 & 0 \\ 0 & 0 & q_{33} & 0 & 0 \\ 0 & 0 & 0 & q_{44} & 0 \\ 0 & 0 & 0 & 0 & q_{55} \end{bmatrix},$$
$$R = \begin{bmatrix} r_{11} & 0 \\ 0 & r_{22} \end{bmatrix} \tag{11}$$

2) The non-domination rule is applied and the initial population of variables is randomly generated.

3) Every variable is converted into diagonal terms of the two matrices Q & R of EKF observer at each time of iteration. Then the diagonal components are sent to the RC-GA-EKF speed observer, and hence the fitness function is obtained. This method gives the fitness evaluation criterion and thus provides solutions for fitness functions.

4) The operators of crossover and mutation are used to get the off-springs. The present population is sorted along with the current off-spring population based on the rule of non-domination. This gives the best individual P_{op} (population size), which is selected for further operations.

5) Steps 3 & 4 are repeated till the maximum iterations are reached. MATLAB coding is applied to optimize RC-GA EKF observer thus, enhancing the performance.

The closed-loop controller comprises the training set: the voltages and currents of the stator (v_d, v_q, i_{sd}, and i_{sq}). This training set makes the EKF observer's input and takes the obtained rotor speed as the target set for getting the RC- GA fitness evaluation. Around 40000 sets of vector generations, training profiles are generated. These profiles have been seen to provide wide speed range operation from low to high speed both during the transient condition and steady-state conditions.

A comparative analysis is made between the trial-and-error method in EKF and RC-GA using simulation and experimental research. Also, this article presents the hardware configuration for implementing the technique above in section IV.

IV. HARDWARE CONFIGURATION FOR REAL-TIME IMPLEMENTATION OF EKF ON SENSORLESS VECTOR CONTROLLED IM

The TMS320F28335 connects the improved EKF observer and process implementation on target DSP [45] for the hardware test. First, the observer is expressed in mathematical form through the CCS toolbox and then it is optimized via the processor and later is transferred to the hardware platform

This step occurs in two parts:

- First, the EKF observer is loaded in the target DSP and the IM model is described in Simulink.
- Second, the IM model comprises the sensorless field-oriented control strategy.

Building the hardware requires a few initial processes.

- The model is built, arranged, simplified, and tested in a Simulink environment. This prevents timing errors. Implementing the observer in this work has 3 sub-blocks: 1) current estimator, 2) rotor flux estimator – rotor flux is estimated from voltage model of IM and 3) parameter estimation as in Fig. 2.
- Fig. 2 represents a framework of the planned estimator on the RCP platform or the so-called hardware co-simulation platform.
- Using the CCS toolbox in the target DSP of Simulink is the next step. Through this the hardware platform for the estimator is set up. An environment of convenience and precision is created to select the data size and allow the same signal to traverse between the hardware blocks built. The inner information of variables and precise computation are two parameters that must be considered achieving the required data size. Time analysis is performed and the instant at which the improved EKF algorithm gets synchronized with the hardware at various stages of the design process is noted.
- In the previous step before synchronization, the EKF algorithm is verified along with the design. In this stage, simulation along with time analysis and co-simulation with hardware is performed. This process validates the performance of the design parameters on the target DSP board.

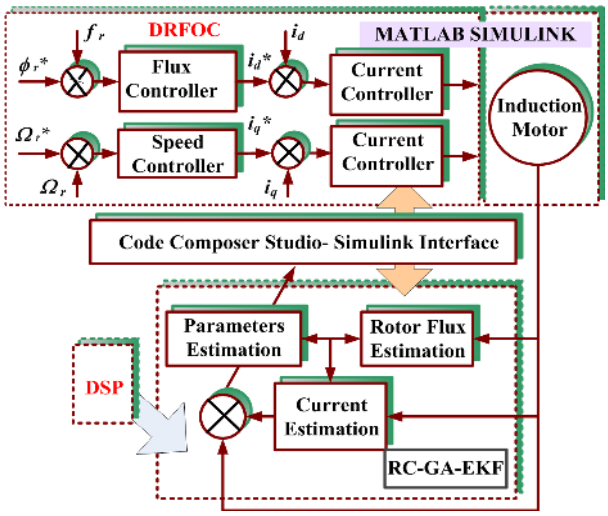

FIGURE 2. Architecture of the proposed estimator.

TMS320F28335 is used for the co-simulation function. A code generator present will synthesize to give a DSP program in C file from the hardware. A new JTAG is used to replace the previously built design (Fig. 2). The block obtained after this is now put in the design. Further, implementation of hardware through the board connected to the PC is performed. In a hardware implementation, the JTAG has a value at one of the input posts and this JTAG now sends the data to the hardware. The hardware provides the estimates and these values are read back to simulation through USB. The output port further functions converting the data type to simulink readable format and further feeds this data to the vector control module (Fig. 2).

To exploit the advantages of the proposed research work, both simulation analysis and experimental analysis are done for diverse working environments of the drive and the estimator, and discussion of results work in section V.

V. RESULTS AND DISCUSSIONS

This section demonstrates the dynamic response of the speed sensorless control scheme of 2 HP IM using RC-GA-EKF.

A. SIMULATION RESULTS

Presented results of the speed response for various load changes. Recorded typical measurements of speed behavior to show the efficacy of the estimation scheme developed in this work. The results show the quality of the speed sensorless control, and relative speed errors. Simulated the sensorless control of IM using GA based EKF on Simulink platform of MATLAB software and study the performance of the observer under different operating conditions. Realization of the model is done using MATLAB language file. Inserts a subsystem into the system that contains the RC-GA-EKF, which is further made into the block as S-function. The RC-GA-EKF in the drive system is implemented for

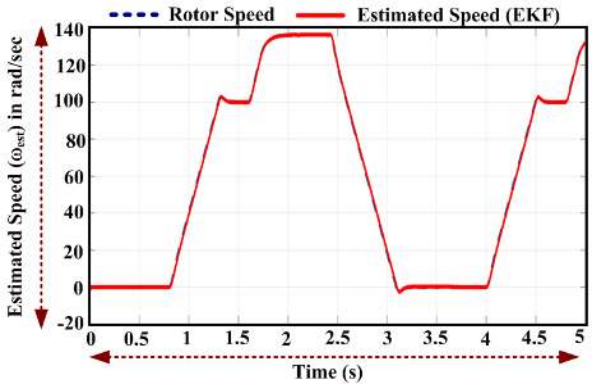

FIGURE 3. Estimation of speed in the high-speed zone of [0 100 139 0] rad/s under no load using improved EKF state observer model of IM.

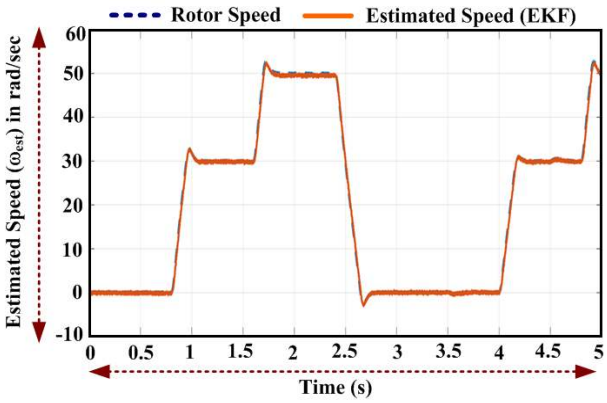

FIGURE 5. Estimation of speed in low speed zone of [0 30 50 0] rad/s, with 10 Nm load using improved EKF.

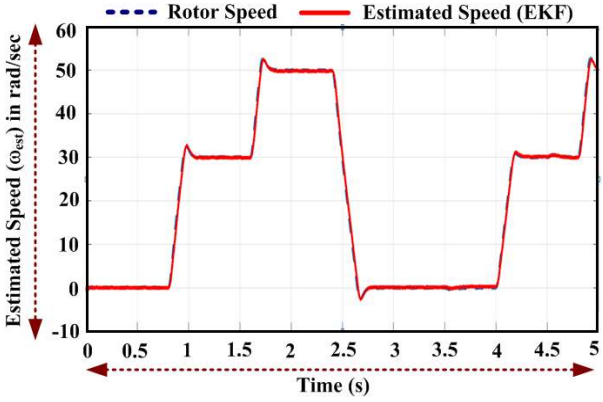

FIGURE 4. Speed estimation in the low speed range of [0 30 50 0] rad/s at no-load using improved EKF state observer model of IM.

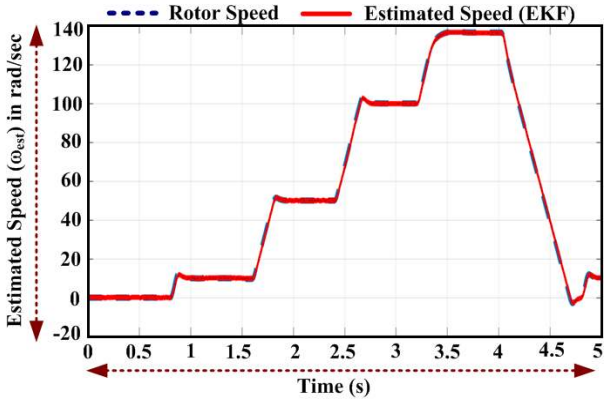

FIGURE 6. Speed Estimation in the range of [0 10 50 100 139 0] rad/s, with 10 Nm load torque using improved EKF.

Pulse Width Modulated inverter driven IM drive without the need of an additional speed sensor. Fig. 3 depicts the speed response of IM at No-load, over a speed range of [0 100 139 0] rad/s. Observed from Fig. 3 that the estimated speed follows the set speed at every step change in speed (the legends in red and blue colors are aligning one over the other). The speed response got in the simulation is steady with minor errors (in the band of [−0.001 to +0.001] as in Fig. 3. It is witnessed that an improved EKF based estimation mechanism overcomes drift and distortion issues that were noticed in MRAS [46], [47] based speed adaptation scheme. An accurate speed estimate at above 100 rad/s (i.e., near rated speed of 139 rad/s) is achieved, as observed in Fig. 3. The performance of the improved EKF at low speeds is entirely satisfactory and the speed. The improved EKF state observer gives better speed estimates even at a low-speed range of [0 30 50] rad/s as shown in Fig. 4, compared to the similar speed range estimates got using the MRAS model [40]. However, the simulation results corresponding to a load torque condition of 10 Nm are presented in this part of the work. The results for different low and high speed values are shown in Fig. 5 and Fig. 6. Fig. 5, shows that the speed estimation obtained is matching with the set speed with an applied load of 10 Nm at an instant of 1 second in a low-speed range which is between 30 and 50 rad/s. The simulation results for a speed range of [0 10 50 100 139] rad/s for 10 Nm load are shown in Fig. 6. It is observed that performing improved EKF is satisfactory over a wide range of speeds. Thus, improved EKF provides a better speed estimate.

To find out the robustness of improved EKF state observer, performed simulation analysis for the effect of 'Current noise' and 'Machine parameter (R_s) changes'. Simulink model of improved EKF observer subjected to noise in stator current and a 10% increase in the value of stator resistance. The noise signal (randomly generated) was injected to show the stator currents of IM in Fig. 7 [40]. The characteristic of the noise is ''zero mean, white and Gaussian''. The estimator's response for a set speed of 30 rad/s is recorded, when a load torque of 10 Nm is applied for 10% variation in the stator resistance of the IM. The nominal value of stator resistance R_s of IM is 4.57 Ω. 10% decrease in the stator resistance applies to performing improved EKF state observer. The result got for a set speed value of 30 rad/s and 139 rad/s Figs. 8 and 9, respectively. Observed that speed estimate tracks the set speed with minimal deviations (± 0.3 rad/s). As shown in Figs. 8 and 9, for low-speed and high-speed range, the computed value of speed is not affected drastically by noise signal injected. From simulation

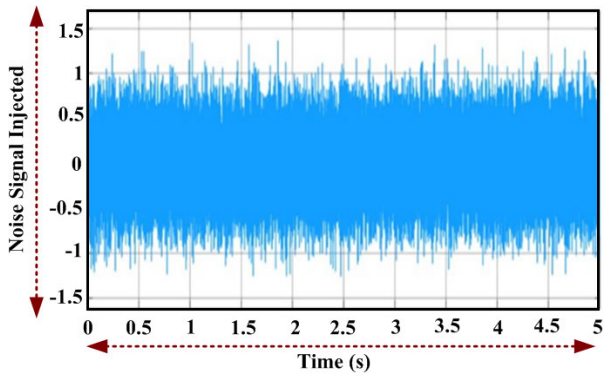

FIGURE 7. Injected noise signal to the stator currents.

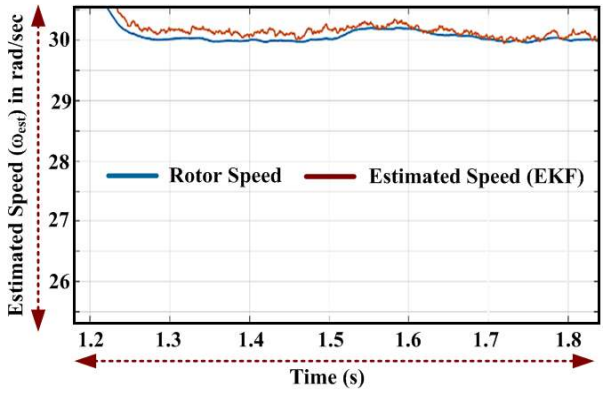

FIGURE 8. Estimated speed curve for speed of 30 rad/s and 10Nm load, 10 % decrease in stator resistance and noise in stator current.

analysis performed, find it that there are almost no differences between the set and the estimated values of speed. Thus, performing the improved EKF model is stable even under the presence of injected noise, variations in stator resistance R_s, and load torque variations. Therefore, the Genetic Algorithm used to tune the state matrices of the EKF state observer, provides a better speed estimate at a widespread speed range, justifying the efficacy of an improved EKF observer. Simulation results presented correspond to a load of 10 Nm and stator resistance variation of 10% of its nominal value. Further, the performing improved EKF is analyzed for load torque variations of 10%, 50%, and 100% of the nominal value (10 Nm) at a common near the rated speed of 139 rad/s. Table 1 show the Mean squared error of speed estimate values got using the 'Trial-and-error' method and improved EKF state estimator. Observed in Table 1 that the Mean squared error of speed estimate recorded for different load torque variations is substantially low compared to the Mean squared error of speed estimate got through the 'Trial-and-error' process. Therefore, the improved EKF speed estimator is proved to perform better than the 'Trial-and-error' scheme of speed estimation. Also, performing improved EKF for stator resistance R_s variation of 10%, 20%, and 50% are analyzed. The nominal value of stator resistance R_s of IM is 4.57 Ω. For a set speed of 139 rad/s (near rated speed) of IM, the mean squared error of speed estimate got upon 10%, 20%, and 50%

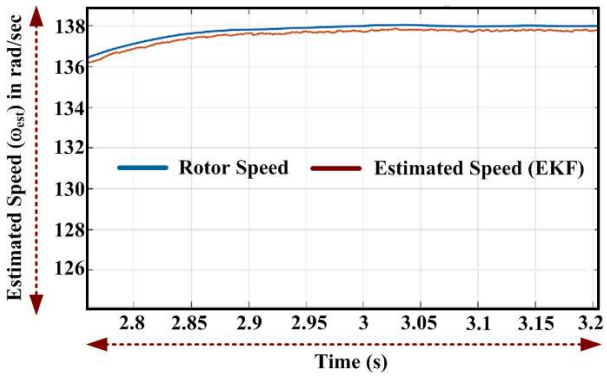

FIGURE 9. Estimated speed curve for speed of 139 rad/s and 10Nm load, 10 % decrease in stator resistance and noise in stator current.

TABLE 1. Mean squared error of speed estimate calculations for load torque variations.

Speed of IM	Load Torque Variation	Mean squared error of speed estimate	
		Trial and error method	Improved EKF
139 rad/s	10%	2.06	1.98
	50%	740.55	4.608
	100%	503.31	0.1105

TABLE 2. Mean squared error of speed estimate calculations for stator resistance variations.

Speed of IM	Stator Resistance R_s Variation	Mean squared error of speed estimate	
		Trial and error method	Improved EKF
139 rad/s	10%	463.61	3.23
	20%	165.25	1.25
	50%	4550	2003

variations of R_s is shown in Table 2. It is observed from the values stated in Table 2 that the mean squared error of speed estimate got through the 'Trial-and-error' method is more sensitive to stator resistance variation than those obtained by improved EKF state observer.

B. SIMULATION ANALYSIS OF RC-GA-EKF STATE OBSERVER APPLIED TO SENSORLESS VECTOR CONTROL OF IM DRIVE

The simulation analysis of sensorless Field Oriented Control (FOC) of the IM using RC-GA-EKF state observer is performed. Sample time of 10e-6s is selected. Fig. 10 shows the generic diagram of a vector control scheme in sensorless mode using an improved EKF state estimator. For a good performance of speed sensorless system accurate rotor speed and flux estimation is necessary. This is because any error in flux estimation can affect the estimated speed and vice versa. Hence, in the presented work, improved EKF is employed only for estimating speed. The flux estimator is used extensively for tracking the position of the rotor-flux linkage. In this subsection, discuss sensorless FOC of the IM

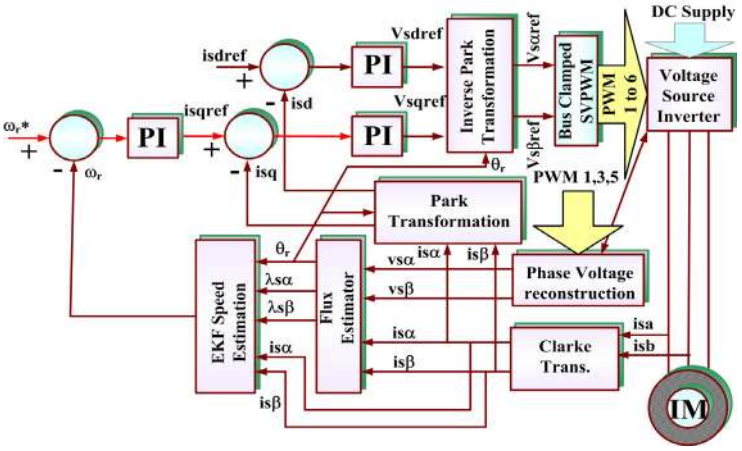

FIGURE 10. Complete structure of RC-GA-EKF speed estimator.

TABLE 3. Values of PI controller used for tuning error signals.

Tuned parameter	K_p	K_I
Current	20	1
Speed	100	1
Flux	1	100

subsequent results. The four PI controllers (flux controller, speed controller, and two current controllers) in the control system are tuned individually by adjusting the proportional constant K_p and the Integral constant K_I.

The gain values of the four PI controllers through the 'Trial-and-error' process. Tuning of these controllers enables the controller error signal to zero. Initially, the inner current loops are tuned (having speed and flux controllers disabled) with constant values of their reference inputs. Later, speed and flux PI controllers are tuned. Table 3 shows the value of K_p and K_I used in this part of the work for the four PI controllers [40]. After tuning the current speed and flux controllers appropriately with the values stated in Table 3, simulation analysis of sensorless vector control for IM is made. The corresponding responses got concerning phase voltage (V_{ab}) in volts, Phase Currents (I_a, I_b, I_c) in amperes, rotor speed in rad/s, electromagnetic torque in Nm, is as in Fig. 11.

Fig. 11 depicts vector control of IM at no load in the sensorless mode for a value of speed 20 rad/s using an improved state observer. It is realized that the estimated speed tracks the reference speed, and the speed estimate is smooth after initial oscillations die down. The initial drift and distortions are because of integrators in PI controllers used for speed control and current control. The performance of the sensorless drive using an improved EKF speed observer is satisfactory when operated under a very low-speed range, between 10 rad/s- 20 rad/s. Attributes the higher amplitude of the transients in stator currents to the inertia of the motor. Observed these amplitudes to decrease drastically by the time the steady-state is reached, as shown in Fig. 11. We make the simulation runs for one load condition of 10 Nm common

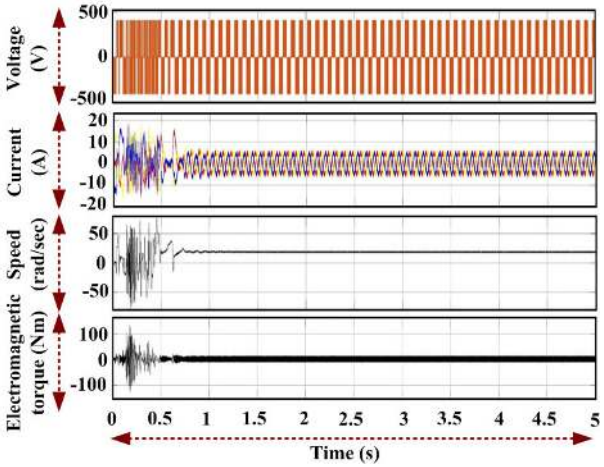

FIGURE 11. IM Vector control operation in sensorless mode under no-load and speed 20 rad/s employing EKF state observer with improved performance.

for two-speed ranges. The low-speed range of [30], [50] rad/s and high-speed 139 rad/s are considered. The responses got in this context are shown in Figs. 12 and 13, respectively. The results got to imply that there are few deviations among the set and estimated speed during load and speed changes in both cases. The conditions realized with such reduced deviations are deemed as a stable operation of sensorless vector control of the IM. It is seen from simulation results, improved EKF overcomes the problem of the MRAS speed estimation scheme for achieving shorter settling time and tuning of PI controller gain value [46], [47]. Therefore, in the present research work, an improved EKF state observer provides accurate speed estimation at a higher speed range. Even at low speeds, even a slight variation in stator resistance does not affect the performance of the drive system. Hence, for high and low-speed estimates in connection with sensorless control of IM, improved EKF stably responds.

Table 4 shows the response of speed sensorless control and relative speed error at different speeds. The measurements for four reference speed settings. The values stated in Table 4

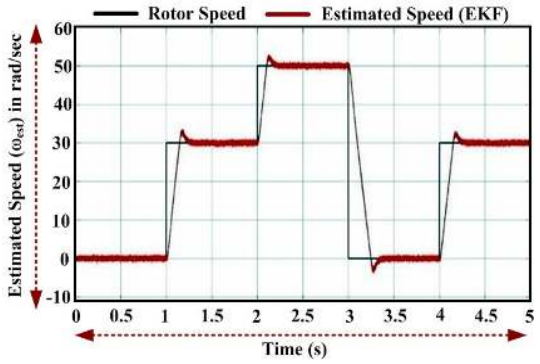

FIGURE 12. Sensorless FOC in low speed range of 30 and 50 rad/s with 10 Nm load.

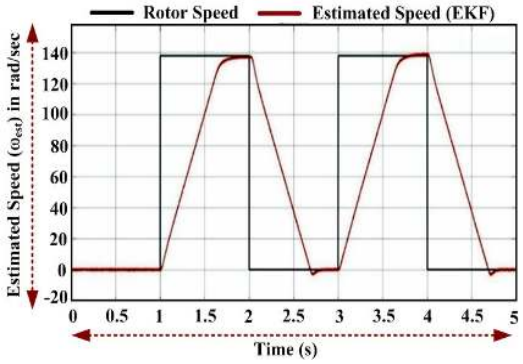

FIGURE 13. Sensorless FOC of IM for speed of 139 rad/s and 10 Nm load.

TABLE 4. Response of speed sensorless control of IM employing improved EKF.

Reference SPEED (rad/s)	Measured speed (rad/s)	Estimated Speed (rad/s)	Speed Control Error (%)
57.5	57.64	57.67	0 .22
86	85.75	85.82	-0 .62
115	114.66	114.82	- 0.33
139	138.8	139.02	0.2

show the efficacy (speed control errors being close to zero) of the control scheme using improved EKF. Thus, accurate speed estimate, sensing, and control are got at an extended speed range, starting from high values of speed down to very low values of speed. Further, the comparative values of speed recordings under no-load condition got through simulation analysis of improved EKF and Model Reference Adaptive System (MRAS) speed estimator are stated in Table 5. The values specified in Table 5 show the capability of improved EKF speed estimator in estimating the rotor speed of IM over a wide speed range demanded. Whereas, the speed estimates using MRAS for high-speed demand like 120 rad/s and 139 rad/s were not at all achieved. Further, comparative analysis of speed estimates got by earlier investigators and made those got in the present research work. The results got under No-load conditions for different ratings of IM and different speed estimation techniques reported in the literature are compared and presented in Table 6. It is observed

TABLE 5. Comparison of speed estimates obtained using MRAS and improved Ekf speed estimators, under no-load condition.

Speed Demand in rad/s	Speed recorded using MRAS based speed estimator in rad/s	Speed recorded using improved EKF speed estimator in rad/s
30	29.6	29.87
60	59.42	59.76
100	98.67	99.02
120	Not achieved	119.23
139	Not achieved	138.75

TABLE 6. Comparison of speed estimates obtained using improved EKF SPEED estimator (Present work) with those reported by earlier investigators, under no-load condition.

Speed Demand in rad/s	Speed recorded using improved EKF speed estimator in rad/s	Zhonggang Yin et. al. [48] 1.1 kW IM	Marut M. et. al. [49] 3.9 kW IM
40	39.87	37	39.6
60	59.76	55.24	58.2
80	78.23	75.54	78.56
100	99.02	95.5	96.23
139	138.75	126.1	132.5

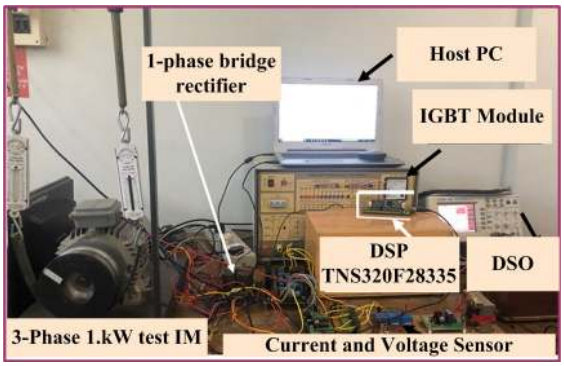

FIGURE 14. Experimental setup for vector control of IM in sensorless mode.

that satisfactory speed estimation is got using improved EKF developed in the present research work. Also, the advantage of the improved EKF speed estimator lies because it does not require 'Change of algorithms' or 'Adjustments of gains' or 'Changing parameter signals' for convergence at a steady state.

The arrived RC-GA-EKF speed estimation algorithm offers a more generalized and effective solution for speed estimation of speed sensorless IM in a wider speed zone.

C. EXPERIMENTATION RESULTS

The performance of improved EKF is tested using hardware setup built as in Fig. 14 for different scenarios of variations in load torque, changes in speed command, no-load conditions, and the worst case of zero speed state [14]. Hardware-in-loop is done by inserting the observer in the controller scheme in the Simulink environment. A generic block diagram depicting the implementation of sensorless vector control using 'hardware co-simulation is shown in Fig. 15. It connects

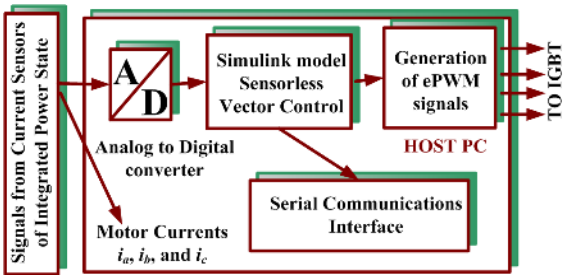

FIGURE 15. Block diagram representing implementation of co-simulation technique for vector control of IM in sensorless mode.

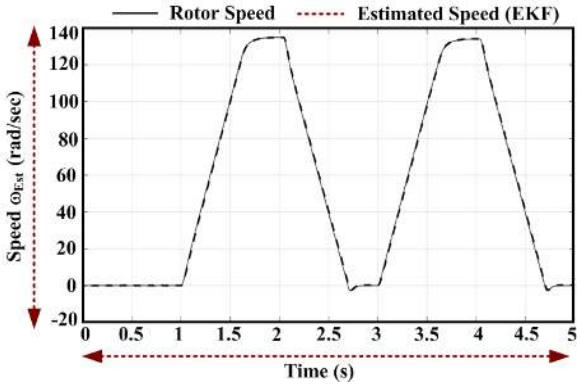

FIGURE 16. Rotor speed estimate at 139 rad/s.

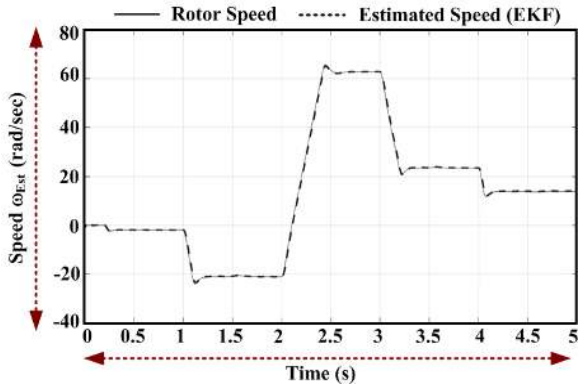

FIGURE 17. Rotor speed estimate at near zero speed rad/s.

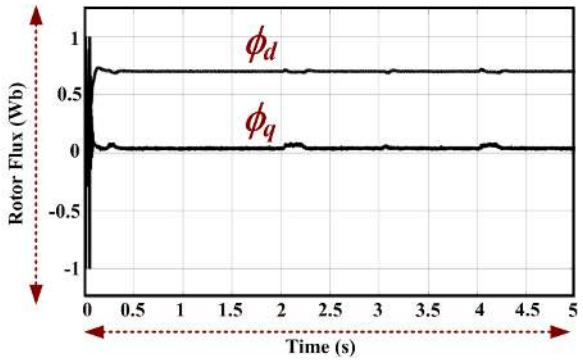

FIGURE 18. Rotor flux linkage obtained through experimental investigation.

DSP TMS320F28335 to the Host PC through USB. Signals from the current sensor of 'Integrated Power State' are provided to Analog-to-Digital Converter (ADC) block got from Embedded coder®Support package for Texas Instruments TMSC2833x Processor. Connected the output of ADC to the Simulink model developed for speed estimation and Sensorless Vector Control of IM. The pulses generated from the Simulink model of Sensorless Vector Control are used to generate ePWM (Enhanced PWM) signals. The ePWM signals provide pulses to drive the IGBT Module. The pulses from the IGBT Power Module further drives the IM to achieve the required speed control. Set the reference phase signal to zero and choose a natural sampling technique for vector control operation. Discretize the induction motor at a sample time of 10 μs.

Current sensors measure the 3-phase current. It transmits all gained data of DSP TMS320F28335 to Host PC through the Serial Communication Interface (SCI) module. The SCI transmit module transfers speed, torque, and current values of IM to the Host PC.

Obtained the data traces of motor currents and speed responses of IM. Checked the suggested estimator under step changes of speed and different load conditions. Results obtained emphasize that when variations are introduced on the parameters estimated, it is observed that the improved EKF gives a good estimation for rotor speed at its rated value of 139 rad/s as shown in Fig. 16. Fig. 17 shows the ability of the improved EKF to sustain its performance at near-zero speed with 80% of load applied to the drive system. From

TABLE 7. Time response analysis of speed response under no-load and loaded condition.

Load Condition	No-load	Load Condition of 1.8 A	Load Condition of 2.2 A (~80% of load)
Delay time	0.32	0.41	0.41
Rise Time	0.20	0.32	0.32
Peak Time	0.5	0.9	0.9
Settling Time	2.2	2	2
Overshoot	6.57	4.26	4.25

the experimental investigation's values of speed at near-zero speed (100 rpm) under load variations are recorded and the corresponding speed error obtained is stated in Table 10. Also, the rotor flux value recorded through the experiment is shown in Fig. 18. The value of the rotor flux remains unaffected even with load and parameter changes. The speed response recorded exhibits good dynamic response both under no-load and loaded conditions. The time response of getting from the speed results is shown in Table 7. Further, compared the time response values stated in Table 8 with the time response got for speed characteristics using the V/f control scheme.

We design both control schemes to operate in the RCP platform for a speed of 1400 rpm under a load current of 1.8 A.

TABLE 8. Time response analysis of speed response under no-load condition for two different speed control techniques.

Load Condition	Sensorless Vector Control using RCP	V/f control using RCP - Sensored Speed Control
Delay time	0.41	0.63
Rise Time	0.32	0.47
Peak Time	0.9	1
Settling Time	2.2	2.5
Overshoot	6.57	7.26

TABLE 9. Speed responses obtained through experimental studies for a set speed of 600 Rpm and different load conditions.

Load Current in A	Measured Speed in rpm	Speed Control Error (%)
0 (No-load)	600	0
1	598.5	0.25
1.4	594.6	0.9
1.8	590	1.6
2.2	588	2.0
2.6 (~80% of rated current)	586	2.3

TABLE 10. Speed responses obtained through experimental studies For different speed ranges and load conditions.

Load Current in A	Set speed in rpm				
	100	500	600	1000	1400
0 (No-load)	100	500	600	1000	1400
1	99	493	598.5	997	1396
1.4	98.2	491	594.6	993.6	1392
1.8	97	489.8	590	991.5	1387
2.2	96.5	487.6	588	990.2	1382
2.6 (~80% of rated current)	95.8	481.7	586	988.2	1375
Avg. Speed control error (in %)	2.25	1.89	1.525	0.6583	0.809

From the responses tabulated; observed that the sensorless vector control scheme provides a better response than the V/f control scheme. Table 9 shows the speed recordings measured for a set speed of 600 rpm under No-load conditions and different load conditions. The rated current of IM is 3.3 A, loading the IM up to ~80% of its rated value (i.e., 2.6 A). We have carried similar investigations out for different set speed values. Table 10 shows the speed recordings made for different speed ranges and load conditions. From the values stated in Table 10, we observe the IM can operate at various speed ranges up to a near rated speed of 1400 rpm with the sensorless vector control scheme. The average speed control error is well within the tolerance band of $\pm$ 2%. This shows better speed regulation. Observed that% error of speed of response decreases as the motor speed increases and is $<$1 at near rated speed. We have presented the comparison of experimental results and simulation results to validate the efficacy of the closed-loop control, and the same is stated in Fig. 19. We record the simulation and experimental results

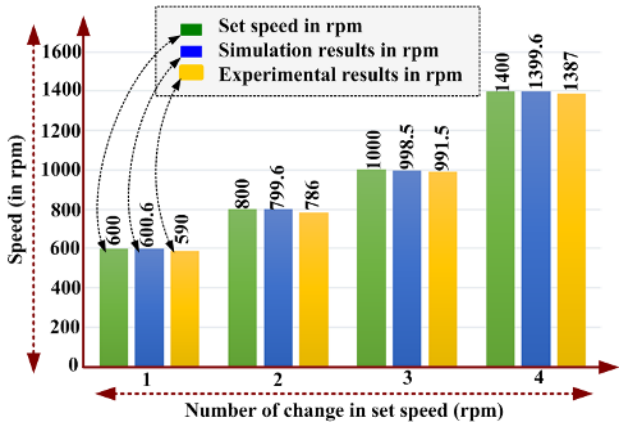

FIGURE 19. Comparison between experimental results and simulation results at a load of 1.8 A.

TABLE 11. Comparison of speed recordings obtained though simulation and experimental investigations in % Error.

Simulation Result in rpm	Experimental results in rpm	% Error
600.6	590	1.76
799.6	786	1.70
998.5	991.5	0.70
1399.6	1387	0.82

for random speed demands of 600 rpm, 800 rpm, 1000 rpm, and 1400 rpm under loaded conditions. The simulation results stand validated upon the experimental results proving the efficacy of the control system designed on the RCP platform. Table 11 presents the percentage difference in speed got between simulation results and experimental results for different speed ranges under loaded conditions. Observed that the % error in speed values well within the tolerance band of $\pm$ 2%.

The results from simulation and experimentation find out that the IM drive-in closed loop operates satisfactorily for different speed and load torque zones. It also reduces the error in speed with load changes and mismatches in parameters of the IM. The transient and steady-state performance of a drive control system is improved. It is observed that results obtained from hardware show fluctuations when compared with results of the simulation environment. This situation depends on the value of the data size chosen. But the fluctuation in the estimated parameter does not have any adverse effect on the dynamic response which does not affect the speed (Fig. 16), and rotor flux (Fig. 18). Neglecting the fluctuations caused during the operation of the drive, results shown in Fig. 17, reports the ability of improved EKF speed observer to sustain its performance at very low speed. Tests validated the proposed work for parameter variations concerning a change in stator resistance and load conditions. We have tested the performance of the algorithm through simulation and experimental results for 50% variations in stator resistance and 100% load variation (through simulation) and 80% load variation through experimental investigations. Under

these conditions, the proposed work has tracked speed at all variations in parameters in the limit described above and has proved less sensitive to any fluctuations in load or parameter variations.

VI. CONCLUSION

In this work, a real-time investigation of a non-linear state observer is done to improve the IM sensorless control in motion control applications by properly estimating the speed of the rotor under changing conditions. Unlike previous studies, where only one of the covariance matrices tuned, the proposed strategy can tune both Q and R matrices and optimize the components of speed and rotor flux. The real coded genetic algorithm based EKF speed observer improves the performance of the sensorless drive system and optimizes the state estimate values the behavior of the system in different zones of speed and load is observed. Results obtained are promising and show that the algorithm has the potential to provide optimal and accurate speed estimates in both low and high-speed ranges.

ACKNOWLEDGMENT

The authors express their gratitude to the Renewable Energy Laboratory (REL), College of Engineering, Prince Sultan University, Riyadh, Saudi Arabia for the technical support received. They would like to acknowledge the support of Prince Sultan University for paying the Article Processing Charges (APC) of this publication.

REFERENCES

[1] M. Rodic and K. Jezernik, "Speed-sensorless sliding-mode torque control of induction motor," *IEEE Trans. Ind. Electron.*, vol. 49, no. 1, pp. 87–95, Feb. 2002.

[2] L. Harnefors, M. Jansson, R. Ottersten, and K. Pietilainen, "Unified sensorless vector control of synchronous and induction motors," *IEEE Trans. Ind. Electron.*, vol. 50, no. 1, pp. 153–160, Feb. 2003.

[3] M. Comanescu and L. Xu, "An improved flux observer based on PLL frequency estimator for sensorless vector control of induction motors," *IEEE Trans. Ind. Electron.*, vol. 53, no. 1, pp. 50–56, Feb. 2006.

[4] R. Bojoi, P. Guglielmi, and G.-M. Pellegrino, "Sensorless direct field-oriented control of three-phase induction motor drives for low-cost applications," *IEEE Trans. Ind. Appl.*, vol. 44, no. 2, pp. 475–481, Mar. 2008.

[5] F. Boldea and S. A. Nasar, *Electric Drives* New York, NY, USA: Taylor and Francis, 2006.

[6] F. Abrahamsen, F. Blaabjerg, J. K. Pedersen, P. Z. Grabowski, and P. Thogersen, "On the energy optimized control of standard and high-efficiency induction motors in CT and HVAC applications," *IEEE Trans. Ind. Appl.*, vol. 34, no. 4, pp. 822–831, Jul. 1998.

[7] J. Holtz, "Sensorless control of induction machines—With or without signal injection?" *IEEE Trans. Ind. Electron.*, vol. 53, no. 1, pp. 7–30, Feb. 2006.

[8] B. Saritha and P. Janakiraman, "Sinusoidal three-phase current reconstruction and control using a DC-link current sensor and a curve-fitting observer," *IEEE Trans. Ind. Electron.*, vol. 54, no. 5, pp. 2657–2662, Oct. 2007.

[9] H. Kim and T. Jahns, "Current control for AC motor drives using a single DC-link current sensor and measurement voltage vectors," *IEEE Trans. Ind. Appl.*, vol. 42, no. 6, pp. 1539–1546, Nov./Dec. 2006.

[10] C. Schauder, "Adaptive speed identification for vector control of induction motors without rotational transducers," *IEEE Trans. Ind. Appl.*, vol. 28, no. 5, pp. 1054–1061, Sep./Oct. 1992.

[11] M. Rashed and A. F. Stronach, "A stable back-EMF MRAS-based sensorless low-speed induction motor drive insensitive to stator resistance variation," *IEE Proc.-Electr. Power Appl.*, vol. 151, no. 6, pp. 685–693, Nov. 2004.

[12] F.-Z. Peng and T. Fukao, "Robust speed identification for speed-sensorless vector control of induction motors," *IEEE Trans. Ind. Appl.*, vol. 30, no. 5, pp. 1234–1240, Sep. 1994.

[13] S. Jafarzadeh, C. Lascu, and M. S. Fadali, "State estimation of induction motor drives using the unscented Kalman filter," *IEEE Trans. Ind. Electron.*, vol. 59, no. 11, pp. 4207–4216, Nov. 2012.

[14] X. Sun, Z. Nie, J. Zhu, Y. Han, and J. Sun, "Speed sensorless control strategy for six-phase linear induction motor based on the dual reduced-dimensional serial extended Kalman filters," *IET Power Electron.*, vol. 12, no. 14, pp. 3758–3766, Nov. 2019.

[15] L. Harnefors and M. Hinkkanen, "Complete stability of reduced-order and full-order observers for sensorless IM drives," *IEEE Trans. Ind. Electron.*, vol. 55, no. 3, pp. 1319–1329, Mar. 2008.

[16] M. J. Lakshmi and H. Suresh, "A robust EKF speed estimator and fuzzy optimization technique for sensorless induction motor drive," *Int. J. Power Electron. Drive Syst.*, vol. 8, no. 1, pp. 147–155, Mar. 2017.

[17] H. K. Khalil, E. G. Strangas, and S. Jurkovic, "Speed observer and reduced nonlinear model for sensorless control of induction motors," *IEEE Trans. Control Syst. Technol.*, vol. 17, no. 2, pp. 327–339, Mar. 2009.

[18] M. Hinkkanen, L. Harnefors, and J. Luomi, "Reduced-order flux observers with stator-resistance adaptation for speed-sensorless induction motor drives," *IEEE Trans. Power Electron.*, vol. 25, no. 5, pp. 1173–1183, May 2010.

[19] S. Bolognani, L. Peretti, and M. Zigliotto, "Parameter sensitivity analysis of an improved open-loop speed estimate for induction motor drives," *IEEE Trans. Power Electron.*, vol. 23, no. 4, pp. 2127–2135, Jul. 2008.

[20] H. Kim, J. Son, and J. Lee, "A high-speed sliding-mode observer for the sensorless speed control of a PMSM," *IEEE Trans. Ind. Electron.*, vol. 58, no. 9, pp. 4069–4077, Sep. 2011.

[21] G. H. B. Foo and M. F. Rahman, "Direct torque control of an IPM-synchronous motor drive at very low speed using a sliding-mode stator flux observer," *IEEE Trans. Power Electron.*, vol. 25, no. 4, pp. 933–942, Apr. 2010.

[22] S. M. Gadoue, D. Giaouris, and J. W. Finch, "Sensorless control of induction motor drives at very low and zero speeds using neural network flux observers," *IEEE Trans. Ind. Electron.*, vol. 56, no. 8, pp. 3029–3039, Aug. 2009.

[23] M. Cirrincione, M. Pucci, G. Cirrincione, and G.-A. Capolino, "Sensorless control of induction machines by a new neural algorithm: The TLS EXIN neuron," *IEEE Trans. Ind. Electron.*, vol. 54, no. 1, pp. 127–149, Feb. 2007.

[24] M. Barut, R. Demir, E. Zerdali, and R. Inan, "Real-time implementation of bi input-extended Kalman filter-based estimator for speed-sensorless control of induction motors," *IEEE Trans. Ind. Electron.*, vol. 59, no. 11, pp. 4197–4206, Nov. 2012.

[25] M. Barut, R. Demir, E. Zerdali, and R. Inan, "Speed-sensorless direct torque control system using bi-input extended Kalman filter for induction motors," in *Proc. Int. Aegean Conf. Electr. Mach. Power Electron. Electromotion, Joint Conf.*, Istanbul, Turkey, Sep. 2011, pp. 343–346.

[26] H. Abu-Rub, J. Guzinski, Z. Krzeminski, and H. A. Toliyat, "Speed observer system for advanced sensorless control of induction motor," *IEEE Trans. Energy Con.*, vol. 18, no. 2, pp. 219–224, Jun. 2003.

[27] B. K. Bose and N. R. Patel, "A sensorless stator flux oriented vector controlled induction motor drive with neuro-fuzzy based performance enhancement," in *Proc. IEEE Ind. Appl. Conf.*, Istanbul, Turkey, Oct. 1997, pp. 393–400.

[28] M. Zerikat, A. Mechernene, and S. Chekroun, "High-performance sensorless vector control of induction motor drives using artificial intelligent technique," *Eur. Trans. Electr. Power*, vol. 21, no. 1, pp. 787–800, Jan. 2011.

[29] M. Barut and R. Demir, "Bi input-extended Kalman filter based speed-sensorless direct torque control of IMs," in *Proc. XIX Int. Conf. Electr. Mach.*, Rome, Italy, Sep. 2010, pp. 6–8.

[30] Y.-R. Kim, S.-K. Sul, and M.-H. Park, "Speed sensorless vector control of induction motor using extended Kalman filter," *IEEE Trans. Ind. Appl.*, vol. 30, no. 5, pp. 1225–1233, Sep. 1994.

[31] H.-W. Kim and S.-K. Sul, "A new motor speed estimator using Kalman filter in low-speed range," *IEEE Trans. Ind. Electron.*, vol. 43, no. 4, pp. 498–504, 1996.

[32] M. Barut, S. Bogosyan, and M. Gokasan, "Speed-sensorless estimation for induction motors using extended Kalman filters," *IEEE Trans. Ind. Electron.*, vol. 54, no. 1, pp. 272–280, Feb. 2007.
[33] M. Barut, S. Bogosyan, and M. Gokasan, "Experimental evaluation of braided EKF for sensorless control of induction motors," *IEEE Trans. Ind. Electron.*, vol. 55, no. 2, pp. 620–632, Jan. 2008.
[34] H. Kubota, K. Matsuse, and T. Nakano, "New adaptive flux observer of induction motor for wide speed range motor drives," in *Proc. 16th Annu. Conf. IEEE Ind. Electron. Soc.*, Dec. 1990, pp. 921–926.
[35] J. Li, L.-H. Zhang, Y. Niu, and H.-P. Ren, "Model predictive control for extended Kalman filter based speed sensorless induction motor drives," in *Proc. IEEE Appl. Power Electron. Conf. Expo. (APEC)*, Mar. 2016, pp. 2770–2775.
[36] Z. Yin, G. Li, X. Sun, J. Liu, and Y. Zhong, "A speed estimation method for induction motors based on strong tracking extended Kalman filter," in *Proc. 8th IEEE Intl. Conf. Power Electron. Motor Control*, Hefei, China, May 2016, pp. 798–802.
[37] E. Zerdali, "Adaptive extended Kalman filter for speed-sensorless control of induction motors," *IEEE Trans. Energy Convers.*, vol. 4, no. 12, pp. 433–436, Aug. 2018.
[38] E. Zerdali and M. Barut, "The comparisons of optimized extended Kalman filters for speed-sensorless control of induction motors," *IEEE Trans. Ind. Electron.*, vol. 64, no. 6, pp. 4340–4351, Jun. 2017.
[39] I. Alsofyani, N. Idris, and K.-B. Lee, "Impact of observability and multi-objective optimization on the performance of extended Kalman filter for DTC of AC machines," *J. Elect. Engg. Tech.*, vol. 14, pp. 231–242, Oct. 2019.
[40] J. Mohana Lakshmi and H. N. Suresh, "Accuracy improvement of induction motor speed estimation using improvised tuning of extended Kalman filter technique," in *Proc. IEEE 13th Int. Conf. Ind. Inf. Syst. (ICIIS)*, Rupnagar, India, Dec. 2018, pp. 395–400.
[41] A. C. Megherbi, H. Megherbi, A. Dendouga, K. Benmahammed, and A. Aissaoui, "Real coded integer genetic algorithm for parameter identification of non linear system," in *Proc. Int. Conf. Commun., Comput. Control Appl. (CCCA)*, Hammamet, Tunisia, Mar. 2011, pp. 1–6, doi: 10.1109/CCCA.2011.6031502.
[42] E. Zerdali and M. Barut, "The optimization of EKF algorithm based on current errors for speed-sensorless control of induction motors," in *Proc. Intl Aegean Conf. Electr. Mach. Power Electron. (ACEMP)*, Side, Turkey, Sep. 2015, pp. 388–392.
[43] N. Salvatore, A. Caponio, F. Neri, S. Stasi, and G. L. Cascella, "Optimization of delayed-state Kalman-Filter-Based algorithm via differential evolution for sensorless control of induction motors," *IEEE Trans. Ind. Electron.*, vol. 57, no. 1, pp. 385–394, Jan. 2010.
[44] K. L. Shi, T. F. Chan, Y. K. Wong, and S. L. Ho, "Speed estimation of an induction motor drive using an optimized extended Kalman filter," *IEEE Trans. Ind. Electron.*, vol. 49, no. 1, pp. 124–133, Feb. 2002.
[45] F. Barbieri, R. P. S. Chandrasena, F. Shahnia, S. Rajakaruna, and A. Ghosh, "Application notes and recommendations on using TMS320F28335 digital signal processor to control voltage source converters," in *Proc. Australas. Univ. Power Eng. Conf.*, Perth, WA, Australia, Sep./Oct. 2014, pp. 1–7.
[46] M. J. Lakshmi and V. H. Pai Suresh, "Non-linear speed estimator and fuzzy control for sensorless IM drive," in *Smart Innovation System and Technology*, vol. 79. Singapore: Springer 2018 pp. 307–317. [Online]. Available: https://link.springer.com/chapter/10.1007/978-981-10-5828-8_30
[47] M. J. and H. N. Suresh, "Sensorless SP experimental evaluation of braided EKF for sensorless control of induction motorseed estimation and vector control of an induction motor drive using model reference adaptive control," in *Proc. Int. Conf. Power Adv. Control Eng. (ICPACE)*, Bengaluru, India, Aug. 2015, pp. 377–382.
[48] R. Inan and M. Barut, "Speed-sensorless direct vector control of induction motor with the EKF based stator resistance estimation on FPGA," in *Proc. Intl Aegean Conf. Electr. Mach. Power Electron. (ACEMP)*, Sep. 2015, pp. 343–347.
[49] M. Tsuji, Y. Umesaki, R. Nakayama, and K. Izumi, "A simplified MRAS based sensorless vector control method of induction motor," in *Proc. Power Convers. Conf.-Osaka*, PCC-Osaka, Japan, 2002, pp. 1090–1095.

MOHANA LAKSHMI JAYARAMU (Senior Member, IEEE) received the B.E. degree from the PES College of Engineering, Mandya, in 2010, the M.Tech. degree from the Malnad College of Engineering, Hassan, in 2012, and the Ph.D. degree in power electronics and drives, in July 2019. She is currently an Assistant Professor with the Department of Electrical and Electronics Engineering, Malnad College of Engineering, Hassan, India. She is a First Rank Holder and a Gold medalist in her M.Tech. programme. She has published several research articles in international journals/conferences. Her research interests include power electronics applied to drive control, electric vehicle technology, and renewable energy systems. She is a Senior Member of the IEEE Education Society, Power Electronics, Industrial Application, and Power and Energy. She has received the Best Project Guide Award for the project titled Fabrication of Potable Solar Water Purifier, in 2018, and the Best Paper Presenter Award for the research article Performance Analysis of 5-level inverter for Hybrid Distribution Generation System. She is a Reviewer Member of various international journals and conferences, including IEEE.

H. N. SURESH received the M.E. degree in electrical engineering and the Ph.D. degree for his computational work titled Modeling of Inhomogeneous Field Breakdown in SF_6 for Lightning Impulse Stress—A Field Approach from the Indian Institute of Science (IISc), Bengaluru, India, in 1991 and 2000, respectively. He is currently working as a Professor with the Malnad College of Engineering, Hassan, India. His research interests include high-voltage insulation engineering, power electronics applied to drive control, and renewable energy sources.

MAHAJAN SAGAR BHASKAR (Senior Member, IEEE) received the bachelor's degree in electronics and telecommunication engineering from the University of Mumbai, Mumbai, India, in 2011, the master's degree in power electronics and drives from the Vellore Institute of Technology, VIT University, India, in 2014, and the Ph.D. degree in electrical and electronic engineering from the University of Johannesburg, South Africa, in 2019. He worked as a Research Student with the Department of Electrical Power Engineering, Power Quality Research Group, Universiti Tenaga Nasional (UNITEN), Kuala Lumpur, Malaysia, in August/September 2017. From 2018 to 2019, he worked as a Researcher Assistant with the Department of Electrical Engineering, Qatar University, Doha, Qatar. He was a Postdoctoral Researcher with his Ph.D. Tutor with the Department of Energy Technology, Aalborg University, Esbjerg, Denmark, in 2019. He is currently with the Renewable Energy Laboratory, Department of Communications and Networks Engineering, College of Engineering, Prince Sultan University, Riyadh, Saudi Arabia. He has authored more than 100 scientific papers particular reference to dc/dc and dc/ac converter, and high gain converter. He is a Senior Member of the IEEE Industrial Electronics, Power Electronics, Industrial Application, and Power and Energy, Robotics and Automation, Vehicular Technology Societies, Young Professionals, various IEEE Councils and Technical Communities. He received the Best Paper Research Paper Awards from IEEE-CENCON'19, IEEE-ICCPCT'14, and IET-CEAT'16, and the IEEE ACCESS Award Reviewer of Month, in January 2019, for his valuable and thorough feedback on manuscripts, and for his quick turnaround on reviews. He is an Associate Editor of *IET Power Electronics*. He is a Reviewer Member of various international journals and conferences, including IEEE and IET.

DHAFER ALMAKHLES (Senior Member, IEEE) received the B.E. degree in electrical engineering from the King Fahd University of Petroleum and Minerals, Dhahran, Saudi Arabia, in 2006, and the master's (Hons.) and Ph.D. degrees from The University of Auckland, New Zealand, in 2011 and 2016, respectively. Since 2016, he has been with Prince Sultan University, Saudi Arabia, where he is currently the Chairman of the Communications and Networks Engineering Department, and the Director of the Science and Technology Unit and Intellectual Property Office, Prince Sultan University. He is the Leader of the Renewable Energy Research Team and Laboratory. His research interests include power electronics, control theory, unmanned aerial vehicles, renewable energy systems, and FPGA applications. He is a member of the IEEE Power Electronics and the IEEE Control Society. He is a Reviewer Member of various international journals and conferences, including the IEEE and IET.

SANJEEVIKUMAR PADMANABAN (Senior Member, IEEE) received the Ph.D. degree in electrical engineering from the University of Bologna, Bologna, Italy, in 2012.

From 2012 to 2013, he was an Associate Professor with VIT University. He joined the National Institute of Technology, India, as a Faculty Member, in 2013. He was invited as a Visiting Researcher with the Department of Electrical Engineering, Qatar University, Doha, Qatar, in 2014, funded by the Qatar National Research Foundation (Government of Qatar). He continued his research activities with the Dublin Institute of Technology, Dublin, Ireland, in 2014. From 2016 to 2018, he worked as an Associate Professor with the Department of Electrical and Electronics Engineering, University of Johannesburg, Johannesburg, South Africa. From March 2018 to February 2021, he has been a Faculty Member with the Department of Energy Technology, Aalborg University, Esbjerg, Denmark. Since March 2021, he has been with the CTIF Global Capsule (CGC) Laboratory, Department of Business Development and Technology, Aarhus University, Herning, Denmark. He has authored over 300 scientific articles.

Dr. Padmanaban is a Fellow of the Institution of Engineers, India, the Institution of Electronics and Telecommunication Engineers, India, and the Institution of Engineering and Technology, U.K. He was a recipient of the Best Paper cum Most Excellence Research Paper Award from IET-SEISCON'13, IET-CEAT'16, IEEE-EECSI'19, IEEE-CENCON'19, and five best paper awards from ETAEERE'16 sponsored Lecture Notes in Electrical Engineering, Springer book. He is an Editor/Associate Editor/Editorial Board for refereed journals, in particular the IEEE Systems Journal, the IEEE Transactions on Industry Applications, IEEE Access, *IET Power Electronics*, *IET Electronics Letters*, and the *International Transactions on Electrical Energy Systems* (Wiley). He is a Subject Editorial Board Member of *Energy Sources—Energies* Journal (MDPI). He is the Subject Editor of the *IET Renewable Power Generation*, *IET Generation, Transmission and Distribution*, and *FACTS* journal (Canada).

UMASHANKAR SUBRAMANIAM (Senior Member, IEEE) worked as an Associate Professor and the Head of VIT Vellore and a Senior Research and Development and a Senior Application Engineer in power electronics, renewable energy and electrical drives. He is currently with the Renewable Energy Laboratory, College of Engineering, Prince Sultan University, Saudi Arabia. He has over 15 years of teaching, research and industrial research and development experience. Under his guidance, 24 master's students and more than 25 bachelor's students completed the senior design project work. Also, six Ph.D. scholars completed Ph.D. thesis as a Research Associate. He is also involved in collaborative research projects with various international and national level organizations and research institutions. He has published over 250 research articles in national and international journals and conferences. He has also authored/coauthored/contributed 12 books/chapters and 12 technical articles on power electronics applications in renewable energy and allied areas. He is a member of IACSIT, IDES, and ISTE. From 2018 to 2019, he has taken charge as the Vice-Chair of the IEEE Madras Section and the Chair of the IEEE Student Activities. He was an Executive Member, from 2014 to 2016, and the Vice-Chair of IEEE MAS Young Professional by the IEEE Madras Section, from 2017 to 2019. He is an Editor of *Heliyon*, an Elsevier journal. He received the Danfoss Innovator Award-Mentor, from 2014 to 2015, and from 2017 to 2018, the Research Award from VIT University, from 2013 to 2018, and the INAE Summer Research Fellowship, in 2014.